ELSEVIER

Journal of Molecular Catalysis A: Chemical 117 (1997) 259–271

JOURNAL OF MOLECULAR CATALYSIS A: CHEMICAL

Study of the catalytical intermediates of metalloporphyrins supported on imidazole propyl gel

Yassuko Iamamoto [a,*], Cynthia M.C. Prado [a], Hérica C. Sacco [a,b], Katia J. Ciuffi [a,b], Marilda D. Assis [a], Ana Paula J. Maestrin [a], Andréa J.B. Melo [a,b], Oswaldo Baffa [a], Otaciro R. Nascimento [c]

[a] *Faculdade de Filosofia Ciências e Letras de Ribeirão Preto, USP, Av. Bandeirantes 3900, CEP 14040-901 Ribeirão Preto, SP, Brazil*
[b] *Instituto de Química, UNESP, Araraquara, SP, Brazil*
[c] *Instituto de Física de São Carlos, USP, São Carlos, SP, Brazil*

Received 19 April 1996; revised 13 August 1996; accepted 13 August 1996

Abstract

In this work, the catalytic intermediates for $Fe(TPP)^+$, $Fe(TDCPP)^+$, $Fe(TFPP)^+$, $Mn(TPP)^+$ and $Mn(TDCPP)^+$ supported on imidazole propyl gel with PhIO were studied by UV–Vis spectrophotometry. For $Fe(TPP)^+$ and $Fe(TFPP)^+$, the study was also monitored by EPR spectroscopy. The active catalytic intermediate observed for FeP–IPG is the oxo-iron (IV) porphyrin π cation radical $Fe^{IV}(O)P^{\cdot+}$, which is evidenced by a decrease in the intensity of the Soret band. The total re-establishment of the initial Soret band intensity for Fe(TDCPP)IPG and Fe(TFPP)IPG at the end of the reaction shows that they were completely recovered. There are advantages in following the reactions of PhIO with unsubstituted $Fe(TPP)^+$ and $Mn(TPP)^+$ on IPG by UV–Vis, since they were slower and allowed to 'see' the intermediate species without spectral interference from the recovered catalyst, since they are only partially recovered. With Fe(TPP)IPG, a band at 580 nm was detected at the beginning of the reaction, indicating the possible formation of a Fe–OIPh intermediate. Supporting $Mn(TPP)^+$ on IPG leads to a shift of band V from 478 nm to 488 nm. In the reaction of MnP–IPG with PhIO, we observed the disappearance of the band in 488 nm and the appearance of a band in 412 nm, which corresponds to the active catalytic intermediate $Mn^V(O)P$ as the main component, as is expected for a more efficient system. The recovery of supported catalysts observed in these experiments was further proved with the possibility of their successive recyclings in cyclohexane oxidation reactions by PhIO.

Keywords: Porphyrins; Metalloporphyrins; Supported intermediates; Intermediates; Imidazole propyl gel

1. Introduction

Porphyrins are important for all organisms [1]. They are indispensable of their function as complexing ligands for catalytically active metal. This relates not only to metabolism, but also to the provision of energy in living creatures and photosynthesis in the plant kingdom [1]. Tetraarylporphyrins, especially iron and manganese complexes with chloro or fluoro substituents, (Fig. 1) can catalyze very similar oxidations to those brought about by cy-

* Corresponding author. Fax: +55-16-6338151; e-mail: iamamoto@usp.br.

PII S1381-1169(96)00362-7

tochrome P-450 and for this reason they have received much attention in recent years. These porphyrins share several of the unusual properties related to catalytic resistance to degradation due to the introduction of electron-withdrawing substituents in the *meso*-aryl position of the tetraphenylporphyrin [2,3].

A logical approach to the design of models for heme proteins might be the attachment of the metalloporphyrin to the support through coordination to ligands on the surface of the silica, since the role of iron protoporphyrin IX in biological oxidations is strongly dependent on the axial ligand to the iron center. The coordinative bond then serves the dual role of anchor and moderator of the metal ion activity [4]. Silica, for example, has been an attractive support for metalloporphyrins, since it is inert even under drastic conditions and has been used as coordinative support by converting its surface silanol groups into silypropyl derivates, which act as ligands [3,4]. The large majority of the studies have employed bound imidazole (Fig. 2) or pyridine [4]. The great advantage of these supported systems is that they consist of hemin in isolated sites, in the same way that the active site of P-450 consists of a protohemin in a

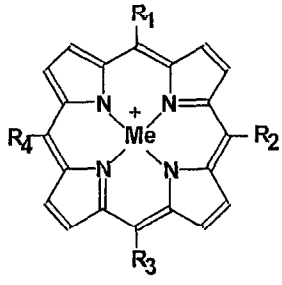

Metalloporphyrin			
1	Fe(TPP)$^+$	$R_1 = R_2 = R_3 = R_4 =$	C_6H_5
2	Fe(TDCPP)$^+$		2,6 diClPh
3	Fe(TFPP)$^+$		C_6F_5
4	Mn(TPP)$^+$		C_6H_5
5	Mn(TDCPP)$^+$		2,6 diClPh
6	Mn(TFPP)$^+$		C_6F_5

Fig. 1. Metalloporphyrins.

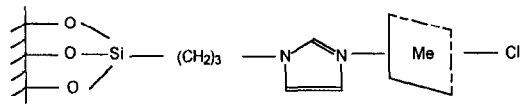

Fig. 2. Metalloporphyrin–IPG.

hydrophobic pocket [5]. The site-isolation on a solid support prevents porphyrin oxidative degradation by bimolecular interaction and/or self-oxidation. The combination of electron-withdrawing substituents in the metalloporphyrins with immobilization on the inorganic supports results in very efficient, selective and easy-to-recover catalysts.

Intensive study of cytochrome P-450 and metalloporphyrins has resulted in a proposed catalytic cycle which involves a high-valent iron-oxo species as the oxygenating agent. Various researchers [6,7] have studied the intermediates for halogenated ironporphyrins (FeP) in homogeneous catalysis. We have also carried out such studies for Fe(TPP)$^+$ [8], mono-*ortho*-nitrophenyl [9] and cationic methylpyridil [10] substitituted FeP. However, up to date there have been no studies about the characterization of intermediates generated from the reaction between electronegatively substituted metalloporphyrins supported on imidazole propyl gel (IPG) and iodosylbenzene (PhIO). This is due to the fact that it is difficult to characterize both the catalyst on the surface of the support and the catalytic intermediates by standard techniques [4]. In this way, it is generally assumed that the behavior of the bound catalyst in the oxidation is the same or similar to that of the homogeneous analog, which can be more readily defined [4]. In this work, the catalytic intermediates (Fig. 1) for Fe(TPP)$^+$ **1**, Fe(TDCPP)$^+$ **2**, Fe(TFPP)$^+$ **3**, Mn(TPP)$^+$ **4**, and Mn(TDCPP)$^+$ **5**, supported on IPG in the reaction with PhIO were studied by UV–Vis spectroscopy and the catalytic intermediates for Fe(TPP)$^+$ **1** and Fe(TFPP)$^+$ **3** supported on IPG with PhIO were studied by EPR spectroscopy.

2. Experimental

2.1. Materials

Dichloromethane (DCM) and 1,2-dichloroethane (DCE) were distilled and stored on 4 Å molecular sieves. Acetonitrile and methanol were stored on 3 Å molecular sieves. *N,N*-dimethylformamide (DMF) was stirred over KOH at room temperature overnight, decanted, then distilled at reduced pressure. Cyclohexane purity was determined by gas chromatographic analysis. Deuterated chloroform ($CDCl_3$) was used as purchased from Aldrich.

2.2. Metalloporphyrins

Commercially available Fe(TPP)Cl, Mn(TPP)Cl, $TDCPPH_2$, and $TFPPH_2$ were purchased from Midcentury. Iron and manganese insertion into the free base porphyrins were done adapting the method described by Adler et al. [11]. DMF was removed by a rotary evaporator and the metalloporphyrins (MePX) obtained were washed with water, which converted them into MePOH, except for **3**, which was converted to the μ-oxo form. The MePOH were purified by silica column chromatography, using for **2**-OH a gradient of a mixture of 5–10% methanol in DCM as eluent, and for **3**-OH or the **3**-μ-oxo form a cyclohexane-DCM 2:3 mixture as eluent. For the purification of **5**-OH, the elution was initiated with 20% methanol in DCM, in order to elute the free base porphyrin first. Then pure methanol was added and the **5**-OH was eluted very slowly, during 48 h. The DCM solution of **5**-OH, **2**-OH and **3**-OH or the **3**-μ-oxo form were bubbled with hydrochloric acid gas, which converted them into **5**-Cl, **2**-Cl and **3**-Cl, respectively.

2.3. Solid supports

Imidazole propyl gel (IPG) was prepared according to the method described by Basolo et al. [12]. Elemental analysis: C = 5.34%, H = 1.20%, N = 0.65%, which corresponds to 2.2×10^{-4} mol of imidazole per gram of IPG (**1**). For the Fe(TDCPP)IPG studies in Fig. 8, another IPG (**2**) with a lower amount of imidazole was prepared and it presented the following elemental analysis result: C = 5.27%, H = 1.05%, N = 0.07%, which corresponds to 2.5×10^{-5} mol of imidazole per gram of IPG.

2.4. Preparation of supported metalloporphyrins (MePIPG)

The metalloporphyrin ligation to IPG was achieved by stirring a DCM solution of a known amount of metalloporphyrin with a suspension of the support for 10–20 min. The resulting supported catalyst was washed with DCM to remove unbound catalyst and weakly bound porphyrin and dried for 3 h at 60°C. The loadings were quantified by measuring the amount of unloaded metalloporphyrin in the combined reaction solvent and washings by UV–Vis spectroscopy.

2.5. Synthesis of iodosylbenzene (PhIO)

It was prepared by the hydrolysis of iodobenzenediacetate [13]. Samples were stored in a freezer and their purity was measured by iodometric assay.

2.6. Hydroxylation reactions

The reactions were carried out in a 2 ml vial with an open top screw cap containing a silicone teflon faced septum. To the vial containing ~ 0.50–2.50 mg of PhIO and 0.0250–0.1000 g of the solid catalyst under argon atmosphere, 100–400 μL of DCE and 100–400 μL of cyclohexane were added. The mixture was stirred at room temperature for the desired time, in the absence of light. The product was extracted with 200 μL aliquots of DCE, followed by 5 min stirring, until 2 mL of extract were

obtained. For the recycling experiments, the catalyst was washed 5 times with 200 μL of DCE. This procedure was done to ensure that the remaining iodosylbenzene was totally removed from the catalyst. This catalyst was then dried for 3 h at 60°C, before the next recycling.

2.6.1. Product analysis

The product was analyzed by gas-chromatography using *n*-octanol as the internal standard. The yields were based on iodosylbenzene. Gas chromatographic analyses were performed on a CG 500 gas chromatograph coupled to a CG-300 integrator, or Varian CX Star chromatograph coupled to workstation operating software. Nitrogen was used as the carrier gas with a hydrogen flame ionization detector. The inox column (length 1.8 m, internal diameter 3 mm) was packed with 10% Carbowax 20M on chromosorb WHP. The attained products were analyzed by comparison of their retention times with authentic samples.

2.7. EPR spectra

The EPR spectra were recorded in a Varian E-109 century line spectrometer operating at the X band. The g values were found by taking the frequency indicated in a HP 5340A frequency meter and the field measured at the spectral features, which were recorded with increased gain and expanded field. Routine calibrations of the field setting and scan were made with DPPH and Cr^{+3} reference signals. The Helitran (Oxford Systems) low temperature accessory was employed to obtain the spectra in the specified temperature range.

2.7.1. Catalytic intermediates of the Fe(TPP)IPG and Fe(TFPP)IPG

The intermediates were generated by adding PhIO in 150 μL of the desired solvent (1.8×10^{-2} mol L^{-1}) to the EPR tube reaction containing the FePIPG suspension in 100 μL of the same solvent (2.2×10^{-4} mol L^{-1}). After stirring for the programmed time the reaction was inhibited by freezing the reaction tube at −77°C (dewar containing dry ice–methanol bath).

2.8. Catalytic intermediates of the MePIPG and PhIO reaction through UV–Vis spectra

Electronic spectra were recorded in a Hewlett-Packard 8452, Diode Array UV–Vis spectrophotometer. For all the experiments, the 'blank' was recorded from a suspension of IPG in the desired solvent at the temperature utilized throughout the whole reaction. All the supported metalloporphyrins studied contained 1.1×10^{-6} mol MeP and 2.2×10^{-4} mol imidazole per gram of IPG, unless otherwise stated.

2.8.1. Fe(TPP)IPG and Fe(TFPP)IPG

A suspension of 0.135 g of **1**–IPG or 0.250 g of **3**–IPG in 500 μL of DCM or $CDCl_3$, respectively, was let to stand in a 2 mm path length quartz cell purchased from Hellma (ref. 220-QS) until the FePIPG was totally sunk. The mass of FePIPG used in the experiment was calculated so that after the sinking process, the height of FePIPG in the cell would guarantee that the FePIPG was in the light path of the spectrophotometer. The cell was transferred to a low temperature UV–Vis Dewar flask from Kontes (ref. 611770) containing methanol previously cooled to −55°C and the spectrum of the suspension of FePIPG was recorded. Afterwards, PhIO in 100 μL DCM or $CDCl_3$ was added to the cell and the mixture was stirred either by ultrasound or manually. The cell was placed back in the optical dewar and the suspension was let to stand again, until the FePIPG was totally sunk. After that spectra were registered at −55°C or −40°C for **1**-IPG and **3**-IPG, respectively. Consecutive spectra were registered for 1 h.

2.8.2. Fe(TDCPP)IPG

Two **2**-IPG containing different amounts of $Fe(TDCPP)^+$ and imidazole were studied: Fe(TDCPP)IPG **1**, containing 1.1×10^{-6} mol

$Fe(TDCPP)^+$ and 2.2×10^{-4} mol imidazole per gram of IPG and Fe(TDCPP)IPG **2**, containing 4.4×10^{-6} mol $Fe(TDCPP)^+$ and 2.2×10^{-5} mol imidazole per gram of IPG. To enable the Soret absorbance reading, it was necessary to 'dilute' **2**-IPG with IPG. This was done by mixing 0.10 g of Fe(TDCPP)IPG **1** or 0.03 g of Fe(TDCPP)IPG **2** with 0.3 g IPG. The mixture was transferred to a cell containing 500 μL DCM and the suspension was let to sink in a dewar containing methanol previously cooled to -70°C for 5 min. The mass of FePIPG used in the experiment was calculated so that after the sinking process the height of FePIPG in the cell would guarantee that the FePIPG was in the light path of the spectrophotometer. Next, the cell was transferred to an optical dewar containing methanol at -25°C and the spectrum of the **2**–IPG suspension was recorded. Then PhIO in 100 μL DCE was added to **2**–IPG, the mixture was stirred manually and the suspension was sunk at -70°C for 5 min. The cell was placed back in the dewar for consecutive spectra registration of the suspension for 1 h.

2.8.3. Mn(TPP)IPG and Mn(TDCPP)IPG

0.10 g of **4**–IPG was 'diluted' with 0.38 g IPG. 0.40 g of diluted **4**–IPG or 0.10 g of **5**–IPG was added to a cell containing 1 mL DCM or 300 μL DCE, respectively. The suspension was let to stand, until the MnPIPG was totally sunk. The mass of MnPIPG used in this experiment was calculated so that the height of MnPIPG in the cell would guarantee that the MnPIPG was in the light path of the spectrophotometer. The cell was transferred to an optical dewar containing methanol at room temperature (25°C) and the spectra of **4**–IPG or **5**–IPG were registered. Next, PhIO in 200 μL DCM or 100 μL DCE was added to **4**–IPG or **5**–IPG, respectively. The mixture was stirred manually and the suspension was let to stand again, until the MnPIPG was totally sunk. The cell was then placed in the optical dewar and consecutive spectra were recorded until complete recovery of the catalyst.

2.9. Catalytic intermediates of the FeTFPPCl and PhIO reaction through UV–Vis spectra

A FeTFPPCl (1.5×10^{-3} mol L^{-1}) solution in $CDCl_3$ was added to a 2 mm path length quartz cell (Hellma) and the cell was transferred to an optical dewar (specially designed for spectra registration at low temperatures) containing methanol previously cooled to -50°C and the spectrum of the solution was recorded. Afterwards PhIO in 100 μL $CDCl_3$ was added to the cell and the mixture was stirred manually. The cell was placed back in the optical dewar for consecutive spectra registration at -55°C for 1 h.

3. Results and discussion

The studies of oxidation reaction intermediates were carried out by EPR and UV–Vis spectroscopy in dichloromethane and deuterated chloroform at different reaction times. The different temperatures at which the spectra were acquired modified the reaction rates and the reaction times considered in each spectroscopic technique cannot be directly related because with UV–Vis spectroscopy the temperature was higher than with EPR measurements.

3.1. Fe(TPP)IPG

There are advantages in studying intermediates with unsubstituted $Fe(TPP)^+$ on IPG monitored by UV–Vis spectroscopy. The rate of the reaction is slower than with the FeP containing electron-withdrawing substituents and so the changes in the spectral patterns allow to identify the species involved. In this way, using the data obtained in Fig. 3, we suggest Scheme 1 as a possible reaction pathway.

The UV–Vis spectrum (Fig. 3A) of the starting catalyst Fe(TPP)IPG, with a Soret band at 418 and a band at 544 nm, indicates a Fe^{III}–imidazole species [14,15], and the corresponding EPR spectrum (Fig. 4A) indicates the presence

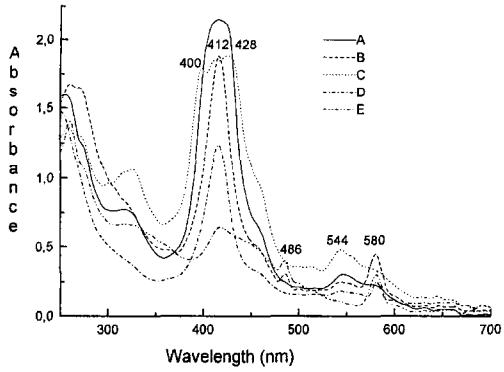

Fig. 3. UV–Vis spectra at −55°C of (A) Fe(TPP)IPG (1.0×10^{-6} mol of FeP and 2.2×10^{-4} mol of imidazole per gram of IPG) in DCM; (B) A after the addition of 100 μL of PhIO in DCM (9.9×10^{-3} mol L^{-1}) and 4 min reaction at −55°C. After 8 min at −55°C the reaction mixture was stirred by ultrasound for (C) 30 s, (D) 43 s, and (E) 1 h.

of Fe^{III} high-spin species. A decrease in the absorbance of the Soret band at 418 nm and its shift to 412 nm is initially observed (Fig. 3B), as well as the appearance of a band at 580 nm, which corresponds to a PFe–O coordination [16]. This band could indicate the formation of the species PFe–OIPh. As the reaction follows (Fig. 3C), the spectrum seems to reflect the coexistence of species I, which presents a broad and less intense Soret band between 400 and 412 nm, and species II, which is characterized by the band at ~428 nm and intensification of the band at 540 nm and is formed through hydrogen abstraction from the solvent by species I [7,8]. The further decrease in the Soret band (~412 nm) and appearance of a band at 580 nm (Fig. 3D) shows that Fe(TPP)IPG is partially recovered and may react with PhIO again. At the end of the reaction (Fig. 3E), a band at 486 nm persists, due to the formation of Fe–O–N species. A possible interconversion between species I and Fe–O–N (which are isoelectronic

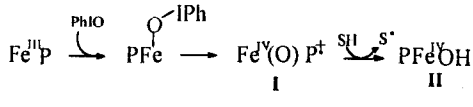

Scheme 1.

species) has been previously reported by us [10] and others [17]:

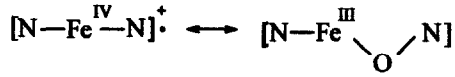

The corresponding EPR spectra confirm the presence of this species (Fe–O–N) (Fig. 4(B–E)), which is known to present an EPR signal at $g = 4.3$ [8–10,18]. This species may be favored with charged FeP [10] and with polar solvent systems [8]. It is related to catalyst destruction once Fe(TPP)IPG recovery is not observed in the UV–Vis spectrum (Fig. 3E), and the $g \sim 4.3$ signal persists at the end of reaction (Fig. 4E).

3.2. Fe(TFPP)IPG

Carrying out the Fe(TFPP)IPG intermediate studies in DCM did not lead to any observable intermediates by UV–Vis spectroscopy because the very electronwithdrawing fluoro-substituents activate the intermediate $Fe^{IV}(O)P^{+\cdot}$, leading to its fast reaction with DCM, similarly to what

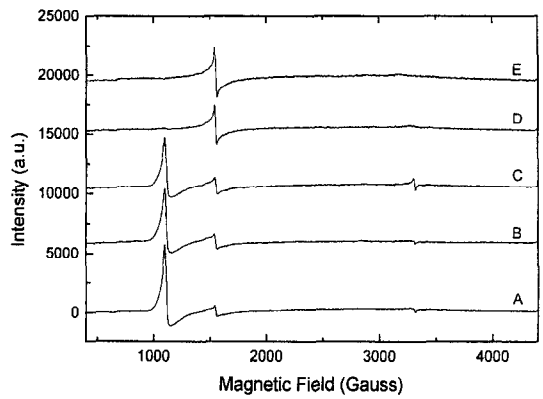

Fig. 4. EPR spectra of (A) Fe(TPP)IPG (0.0530 g of IPG containing 1.0×10^{-6} mol FeP and 2.2×10^{-4} mol imidazole per gram of IPG in DCM; (B) A after addition of 150 μL of PhIO in DCM (1.8×10^{-2} mol L^{-1}); (C) reaction B after 105 s of manual stirring; (D) C after 24 min of manual stirring; (E) D after 12 min of ultrasound stirring and 3 h and 45 min at 25°C. EPR spectrometer conditions: temperature of 4–5 K, microwave power of 4 mW, modulation amplitude 4.0 G, microwave frequency 9.240 GHz and gain 1.0×10^{4}.

occurs with Fe(TDCPP)Cl in a solution system [19,20]:

$$Fe^{IV}(O)P^{\cdot+} + CH_2Cl_2 \rightarrow Fe^{IV}(OH)P + Cl_2HC^{\cdot}$$
$$\rightarrow Fe^{III}P + HC(O)Cl + HCl$$
$$Fe^{IV}(O)P^{\cdot+} + HC(O)Cl \rightarrow Fe^{III}P + CO_2 + HCl$$

Therefore we decided to use $CDCl_3$ as reaction solvent (Fig. 5). The starting Fe(TFPP)IPG spectrum (Fig. 5A) indicates a mixture of species. It is possible that Fe^{II} is present, and the corresponding Soret band is displaced to higher wavelength exhibiting a shoulder at 422 nm, which is in agreement with $Fe^{II}P$ species [8–10]. The dimer species may also be present if one considers that this FeP has a great tendency to dimerize [16,21,22]. The band at 408 nm may be the result of the overlap of the Soret bands corresponding to the following species: $Fe^{II}P$–IPG (λ_{max} = 420 nm), $Fe^{III}P$–IPG (λ_{max} = 420 nm) and PFe^{III}–O–$Fe^{III}P$–IPG (λ_{max} = 398 nm). The dimeric species may have been formed in solution immediately before the anchoring of the FeP on the support. In the EPR spectrum (Fig. 6A), the starting FeP shows a relatively small $Fe^{III}P$–imidazole high-spin signal at $g \sim 6$, while at the end of the reaction this signal is increased to 220% (Fig. 6D), indicating that an EPR silent FeP was converted

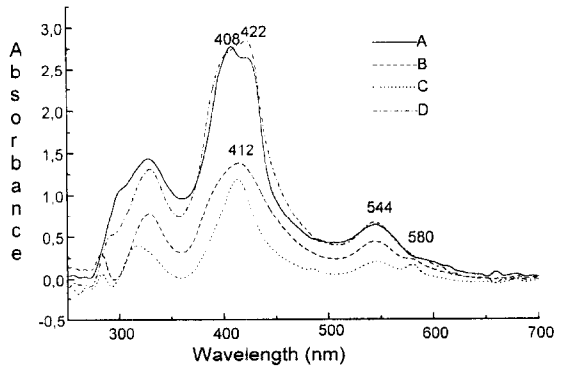

Fig. 5. UV–Vis spectra at −40°C of (A) Fe(TFPP)IPG (1.0×10^{-6} mol of FeP and 2.2×10^{-4} mol of imidazole per gram of IPG) in $CDCl_3$. After the addition of 100 μL of PhIO in $CDCl_3$ (5.1×10^{-3} mol L^{-1}), the reaction mixture was stirred for 25 min and the reaction was left at 25°C for (B) 100 min, (C) 114 min, and (D) 230 min.

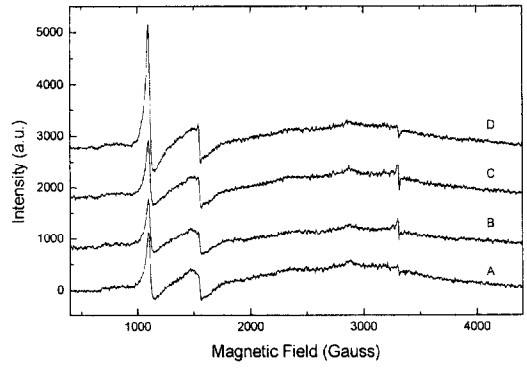

Fig. 6. EPR spectra of (A) Fe(TFPP)IPG (0.0530 g of IPG containing 1.0×10^{-6} mol FeP and 2.2×10^{-4} mol imidazole per gram of IPG in $CDCl_3$; (B) A after the addition of 150 μL of PhIO in $CDCl_3$ (1.8×10^{-2} mol L^{-1}); (C) reaction B after 45 s of manual stirring and 65 s of ultrasound stirring; (D) C after 45 min of ultrasound stirring. EPR spectrometer conditions: temperature of 4–5 K, microwave power of 4 mW, modulation amplitude 4.0 G, microwave frequency 9.240 GHz and gain 1.0×10^{4}.

to $Fe^{III}P$ high-spin species. One EPR silent species could be PFe^{III}–O–$Fe^{III}P$–IPG, which can monomerize during the long time used for ultrasound stirring in the experiment. Another EPR silent species could be $Fe^{II}P$–IPG, which may be oxidated to $Fe^{III}P$–IPG during the ultrasound stirring process. In the case of Fe(TFPP)IPG we did not observe the formation of $Fe^{IV}POH$ (species II) through UV–Vis spectra, and the decrease in the Soret band at 412 nm showed in the spectrum in Fig. 5B gives evidence that $Fe^{IV}(O)P^{\cdot+}$ (species I) predominates. This same decrease in the Soret band was observed in the reaction between Fe(TFPP) and PhIO in homogeneous solution (Fig. 7), where the active species $Fe^{IV}(O)P^{\cdot+}$ was also generated [22,23]. As is expected with this stable FeP, the 486 nm band is not evident at the end of the reaction and the spectrum in the Fig. 5D indicates the recovery of the FeP.

3.3. Fe(TDCPP)IPG

To better understand the results attained for Fe(TDCPP)IPG **1** and **2** (Table 1) in the study of the catalytical intermediates, we will first develop a discussion about its catalytic activity

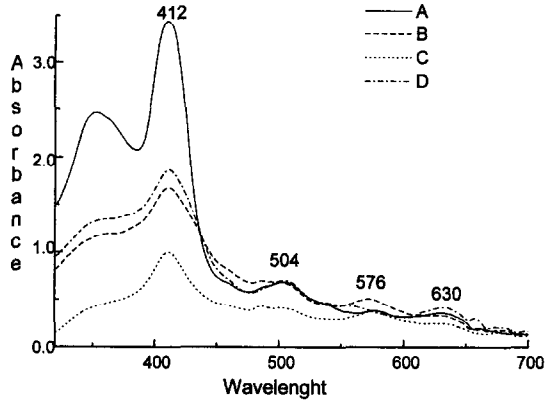

Fig. 7. UV–Vis spectra at −55°C of (A) Fe(TFPP)Cl (1.5×10^{-3} L^{-1}) in $CDCl_3$. After the addition of 100 μL of PhIO in $CDCl_3$ (9.9×10^{-3} mol L^{-1}) and (B) 10 s; (C) 15 s and (D) 1 h of manual stirring.

and characterization through spectroscopic techniques. In Table 1, the yields of cyclohexanol attained in the hydroxylation of cyclohexane by PhIO, having Fe(TDCPP)IPG **1** or **2** as catalyst, are presented [14,15]. We have already reported that the UV–Vis spectrum of Fe(TDCPP)IPG **1**, with absorption bands at $\lambda = 420$ nm (Soret) and 552 nm, indicates that $Fe(TDCPP)^+$ coordinates to IPG through the imidazole groups [14,15]. To find out whether $Fe(TDCPP)^+$ is mono- or bis-ligated to the support and to gain insight into the iron oxidation and spin states, Fe(TDCPP)IPG **1** and **2** were characterized by EPR [14,15].

Fe(TDCPP)IPG **1** presented weak EPR signal in $g_z = 2{,}983$ and $g_y = 2{,}299$ (g_x not determined) due to the presence of low-spin Fe^{III} species [14]. This indicates that $Fe(TDCPP)^+$ bis-coordinates to the imidazole groups in IPG. In this same work [14], we reported that when excess imidazole is added to Fe(TDCPP)IPG **1**, the low-spin Fe^{III} signals decrease, indicating that the reduction Fe^{III} to Fe^{II} may have occurred. We thought then, that besides low-spin Fe^{III}, Fe(TDCPP)IPG **1** might also contain Fe^{II} species. To confirm such a suggestion, we carried out the titration of Fe(TDCPP)IPG **1** with NO [15], which functions as paramagnetic probe [24,25] and through such a study, the presence of Fe^{II} species in this catalyst was confirmed. Recently, Lindsay-Smith [26] also reported the confirmation of the presence of $Fe^{II}P$ in Fe(TDCPP)Si–Py (support = silica gel functionalized with pyridine) using CO. In this way, it was possible to understand why the catalytic activity of Fe(TDCPP)IPG **1** is relatively low. (Col (%) = 28, Table 1). The active species $Fe^{IV}(O)P^{\cdot+}$, which is thought to be responsible for the oxidation of cyclohexane, is generally formed from high-spin Fe^{III} species. As the latter is not present in Fe(TDCPP)IPG **1**, $Fe^{IV}(O)P^{\cdot+}$ may be being slowly formed from low-spin $Fe^{III}P$, while $Fe^{II}P$ does not lead to the oxo-ferril π-cation radical species. The low-spin $Fe^{III}P$ species react slowly with PhIO to furnish $Fe^{IV}(O)P^{\cdot+}$ species because it is bis-coordinated to the support, which makes the approach between FeP and PhIO difficult. Such suggestion was further confirmed through the studies of

Table 1
EPR signals and catalytic activity in cyclohexane oxidation of various Fe(TDCPP)IPG

Catalyst	mol $Fe(TDCPP)^+$/g IPG	mol Im/g IPG	Im/$Fe(TDCPP)^+$	C-ol (%) [a]	EPR signals
Fe(TDCPP)IPG 1	1.1×10^{-6}	2.2×10^{-4}	2.0×10^{2}	28	$g_z = 2.983$ $g_y = 2.299$
Fe(TDCPP)IPG 2	4.5×10^{-6}	2.2×10^{-5}	4.9	67	$g_z = 2.983$ $g_y = 2.299$ $g = 5.878$

Conditions: Argon atmosphere; $T = 25$°C; PhIO/$Fe(TDCPP)^+$ molar ratio = 17; magnetic stirring;reaction time = 1 h; solvent for reaction suspension and product extraction: 1,2-dichloroethane.

[a] Error average of 3%, based on the starting PhIO. C-ol = cyclohexanol.

catalytic intermediates generated from the reaction between Fe(TDCPP)IPG **1** and PhIO (Fig. 8).

With Fe(TDCPP)IPG **2**, higher amounts of $Fe(TDCPP)^+$ and imidazole in the support gave rise to EPR high-spin Fe^{III} signals at $g = 5.9$ and better cyclohexanol yields were obtained with this catalyst (Col (%) = 67, Table 1) [14,15]. This confirms that the formation of $Fe^{IV}(O)P^{\cdot+}$ species depends on the presence of high-spin $Fe^{III}P$ on the supported catalyst. The spectra recorded for such studies are presented in Fig. 9.

To follow the discussion below, we must remember that, to enable the reading of the Soret band, both Fe(TDCPP)IPG **1** and **2** were 'diluted' with IPG, leading to a final amount of $4{,}0 \times 10^{-7}$ mol $Fe(TDCPP)^+$ per gram of IPG in both cases (item 2.8). With Fe(TDCPP)IPG **1**, a decrease of 12% in the intensity of the Soret band ($\lambda = 418$ nm) was observed upon addition of PhIO (Fig. 8B), which is an evidence of the formation of the $Fe^{IV}(O)P^{\cdot+}$ species. The characterization of Fe(TDCPP)IPG **1** by EPR had indicated that it contains Fe^{III} only in the low-spin form [14,15]. Therefore, this intermediate study indicates that it is possible to originate $Fe^{IV}(O)P^{\cdot+}$ from low-spin Fe^{III} species.

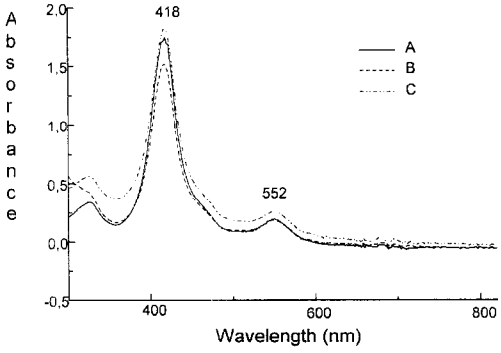

Fig. 8. UV–Vis spectra at −25°C of (A) Fe(TDCPP)IPG **1** (1.0×10^{-6} mol of FeP and 2.2×10^{-4} mol of imidazole per gram of IPG) in dichloromethane; (B) after the addition of 100 μL of PhIO in DCM (2.0×10^{-2} mol L^{-1}) and 6 min reaction at −25°C; (C) reaction B after 1 h reaction at −25°C and 5 s ultrasound stirring at +25°C.

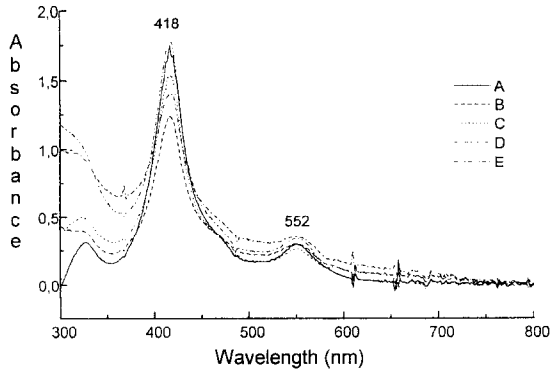

Fig. 9. UV–Vis spectra at −25°C of (A) Fe(TDCPP)IPG **2** (4.4×10^{-6} mol of FeP and 2.2×10^{-5} mol of imidazole per gram of IPG) in dichloromethane; (B) after the addition of 100 μL of PhIO in DCM (2.6×10^{-2} mol L^{-1}) and 6 min reaction at −25°C; (C) B after 40 min reaction at −25°C; (D) C after 15 s manual stirring at +25°C; (E) D after 5 s ultrasound stirring at +25°C.

With Fe(TDCPP)IPG **2**, a decrease of 30% in the intensity of the Soret band ($\lambda = 418$ nm) is observed upon addition of PhIO (Fig. 9B), which gives evidence of the formation of $Fe^{IV}(O)P^{\cdot+}$. Remembering that when we diluted both Fe(TDCPP)IPG we had obtained the same amount of $Fe(TDCPP)^+$ per gram of IPG, comparing the initial absorption of their Soret band, we have 1.75 for both catalysts (Fig. 8A and Fig. 9A). However, after reaction with PhIO, the decrease in the Soret band is more pronunciated for Fe(TDCPP)IPG **2**. In fact, the characterization of this catalyst through EPR gave indication that Fe(TDCPP)IPG **2** contains a greater amount of Fe^{III} species than Fe(TDCPP)IPG **1** [14,15]. As it contains more Fe^{III} and because the formation of the catalytic intermediate species is faster from high-spin $Fe^{III}P$, Fe(TDCPP)IPG **2** gives rise to a greater amount of $Fe^{IV}(O)P^{\cdot+}$ species, leading to better catalytic results than Fe(TDCPP)IPG **1** (Col (%) = 67 and 28, respectively; Table 1).

After 40 min of reaction, part of the Fe(TDCPP)IPG **2** catalyst is already recovered (Fig. 9C). We then stirred the reaction manually after 40 min and registered a new spectrum. A further decrease in the Soret band was observed, indicating that the catalyst reacted with PhIO

again to form $Fe^{IV}(O)P^{\cdot+}$ (Fig. 9D). In the end of the experiment, the mixture was stirred by ultrasound. At this time, a total recovery of Fe(TDCPP)IPG **2** (Fig. 9E) was obtained. This also happened to Fe(TDCPP)IPG **1** (Fig. 8E) We think that ultrasound promoted the reaction between the active species $Fe^{IV}(O)\ P^{\cdot+}$ and the solvent DCM (reaction I), leading to the total recovery of the initial $Fe^{III}P$ [20].

3.4. Mn(TPP)IPG and Mn(TDCPP)IPG

Supporting $Mn(TPP)^+$ on IPG leads to a shift of band V from 478 nm to 488 nm. In Fig. 10A and Fig. 11A, the differences between the positions of the UV–Vis band observed for $Mn^{III}P$–IPG compounds ($\lambda_{max} = 488$ nm) and $Mn^{V}(O)P$ or $Mn^{IV}(O)P$ ($\lambda \sim 409$–416 nm) have allowed us to follow the transfer of the oxygen atom from PhIO to the MnP complex, to form a manganese–oxo porphyrin. When the reaction of the catalyst Mn(TPP)IPG with PhIO in DCM is monitored by UV–Vis spectroscopy, we observe the disappearance of the band at 488 nm, which means that the $Mn^{III}P$ is being consumed. The disappearance of $Mn^{III}P$ is accompanied firstly by the formation of a band at 409 nm (Fig. 10B). In a study described by us elsewhere

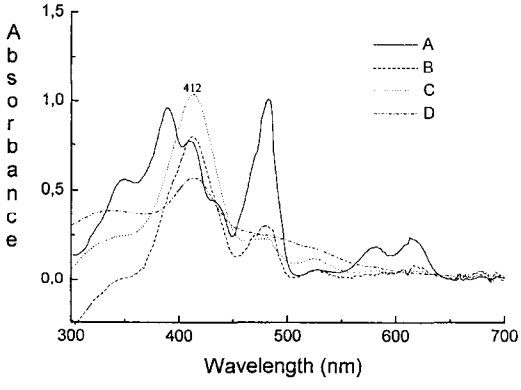

Fig. 10. UV–Vis spectra at 25°C of (A) Mn(TPP)IPG (1.0×10^{-6} mol of MnP and 2.2×10^{-4} mol of imidazole per gram of IPG) in dichloromethane; (B) after the addition of 100 μL of PhIO in DCM (9.9×10^{-3} mol L^{-1}) after 1 min reaction at 25°C; (C) after 7 min reaction at 25°C; (D) after 58 min reaction at 25°C.

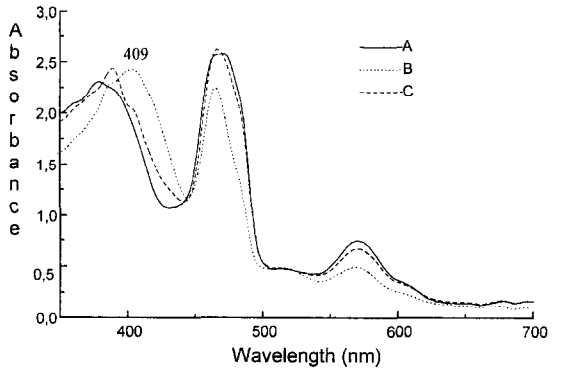

Fig. 11. UV–Vis spectra at 25°C of (A) Mn(TDCPP)IPG (1.0×10^{-6} mol of MnP and 2.2×10^{-4} mol of imidazole per gram of IPG) in dichloromethane; (B) after the addition of 100 μL of PhIO in DCM (9.9×10^{-3} mol L^{-1}) after 2 min reaction at 25°C; (C) after 52 min reaction at 25°C.

[27], a similar reaction in a homogeneous system was monitored by UV–Vis spectroscopy and there was indication that a mixture of the species $Mn^{IV}(O)P$ and $Mn^{V}(O)P$ was present. The deconvolution of the spectrum indicated two components: one with λ_{max} at 408 and another with λ_{max} at 430 nm, which were assigned to $Mn^{V}(O)P$ and $Mn^{IV}(O)P$ species, respectively [27]. So the band in 409 nm in the spectrum of Mn(TPP)IPG can be attributed to a mixture of species $Mn^{V}(O)P$ and $Mn^{IV}(O)P$ (in a minor amount), as has been reported in the literature for the analog homogeneous system [27,28]. After 7 min of reaction, the band at 409 nm shifts to 416 nm, indicating the disappearance of the $Mn^{V}(O)P$ species (Fig. 10C) and the $Mn^{IV}(O)P$ species persists after 1 h of reaction (Fig. 10D). It has been known that $Mn^{IV}(O)P$ is relatively stable when compared to $Mn^{V}(O)P$ [29]. The $Mn^{IV}(O)P$ remains in solution for several hours. It is known that $Mn^{V}(O)P$ is the active intermediate species responsible for the selective cyclohexane hydroxylations [14,15,30]. In this way, for the Mn(TPP)IPG system, when the intermediate active species $Mn^{V}(O)P$ is formed, oxygen transfer to the substrate promptly occurs. In this case, the substrate is solvent DCM, as in the case of FeP–IPG systems (reaction I). Considering Mn(TPP)IPG a

Table 2
Catalytic activity of metalloporphyrins supported on IPG in the recycling experiments for cyclohexane hydroxylation

	Cyclohexanol yield (%) [a]				
	FeTPP	FeTDCPP 2 [b]	FeTFPP [c]	MnTPP	MnTDCPP [c]
Unused catalyst	22	83	63	42	67
First recycle	10	77	46	21	78
Second recycle	0	76	46	20	47
Third recycle	77	46	20	38	38
Fourth recycle		65	16	0	38
Fifth recycle		73	16		38

Conditions: 1.1×10^{-6} mol of metalloporphyrins per gram of IPG; 2.2×10^{-4} mol of imidazole per gram of IPG; magnetic stirring for 1 h, PhIO:catalysts molar ratio: 17 to 20:1, except for FeTFPP, for which it was 80:1; solvent for reaction suspension and product extraction: 1,2-dichloroethane.

[a] Error average of 3%, based on the starting PhIO.

[b] 4.4×10^{-6} mol $Fe(TDCPP)^+$ per gram of IPG; 2.2×10^{-5} mol imidazole per gram of IPG.

[c] Ref. [14,15].

not too stable system we cannot observe significant $Mn^{III}P$ catalyst recovery.

For Mn(TDCPP)IPG, the first active species formed after 2 min of reaction is $Mn^{V}(O)P$ (Fig. 11B), identified by the band at 409 nm. Even though the $Mn^{V}(O)P$ species is formed, the 488 nm $Mn^{III}P$ band becomes lower without disappearing. At 52 min of reaction, the catalyst seems to be totally recovered (Fig. 11C). The recycling experiments (Table 2) were also in agreement with the higher stability of Mn(TDCPP)IPG.

Comparing the catalytic results obtained with MnP in homogeneous and heterogenized systems in the oxidation of cyclohexane by PhIO (Table 3), one can observe that MnPIPG lead to higher yields and selectivity for cyclohexanol. It is known in the literature [14,15,30] that imidazole as axial ligands in MnP favor the formation of the $Mn^{V}(O)P$ species. In fact, it was observed by our group that $Mn(TDCPP)^+$ in a homogeneous system leads to the preferential formation of $Mn^{IV}(O)P$, and only a small amount of $Mn^{V}(O)P$ species is formed [27], which results in low yields of cyclohexane hydroxylation (Table 3). The higher yields and selectivity attanained with MnPIPG systems show that imidazole present on the support favors the formation of the active species $Mn^{V}(O)P$, as was evidenced by the UV–Vis spectra (Figs. 10 and 11). This is the species responsible for the fast oxygen transfer to cyclohexane.

Table 3
Catalytic activity of MnP in a homogeneous system and supported on IPG in cyclohexane hydroxylation

Catalyst	Solution		IPG	
	C-ol (%)	C-one (%)	C-ol (%)	C-one (%)
$Mn(TPP)^+$	19	7	38	—
$Mn(TDCPP)^+$	17	4	68	—

Conditions: 1.1×10^{-6} mol of metalloporphyrins per gram of IPG; 2.2×10^{-4} mol of imidazole per gram of IPG; $[MnP^+] = 5.0 \times 10^{-4}$ mol L^{-1}, magnetic stirring for 1 h, PhIO:catalyst molar ratio of 20:1; solvent: 1,2-dichloroethane. Yields based on the starting PhIO, error average of 3%. C-ol = cyclohexanol, C-one = cyclohexanone.

4. Conclusions

The active catalytic intermediate observed for FeP–IPG is the oxo-iron (IV) porphyrin π cation radical $Fe^{IV}(O)P^{\cdot+}$, which is evidenced by a decrease in the intensity of the Soret band. The total re-establishment of the initial Soret band intensity for Fe(TDCPP)IPG and Fe(TFPP)IPG at the end of the reaction shows that they were completely recovered.

In the reaction of MnP–IPG with PhIO, we observed the disappearance of band V at 488 nm and the appearance of a band at 412 nm,

which corresponds to the active catalytic intermediate $Mn^{V}(O)P$ as the main component, as is expected for a more efficient system.

The total recovery of the supported metalloporphyrins bearing electronwithdrawing substituents in the *meso*aryl positions of the porphyrin ring was further proved with the possibility of their successive recyclings in cyclohexane oxidation reactions by PhIO (Table 2). In fact, Lindsay-Smith et al. [31] have already reported very good results and high turnovers for this same kind of catalysts in epoxidation reactions.

MeP–IPG containing electronwithdrawing substituents present great advantages concerning catalyst resistance and efficiency. However, in these studies, the high reaction rates in these systems do not allow one to 'see' all the intermediate species, as was possible with the unsubstituted Fe(TPP)IPG. In the UV–Vis study, for example, the spectrum of the fast recovered catalyst overlaps that of the intermediate species in the cases of Fe(TDCPP)IPG and Fe(TFPP)IPG, while for Fe(TPP)IPG, it was possible to observe the formation of a Fe^{III}–OIPh species.

Therefore, although unsubstituted MeTPP led to low yields of cyclohexanol, when compared to the substituted MeP, they were a good probe to detect various catalytic intermediate species.

Acknowledgements

We thank FAPESP, CNPq and CAPES for financial support, E.J. Nassar for technical assistance and O.A. Serra for helpful discussions.

References

[1] A.L. Lehninger, Princípios de Bioquímica (Sarvier, São Paulo, 1988); B. Franck and A. Nonn, Angew Chem. Int. Ed. Engl. 34 (1995) 1795, and references therein.

[2] P.S. Traylor, D. Dolphin and T.G. Traylor, J. Chem. Soc. Chem. Commun. (1984) 279; C.K. Chang and F.J. Ebina, J. Chem. Soc. Chem. Commun. (1981) 778.

[3] B. Meunier, Chem. Rev. 92 (1992) 1411.

[4] J.R. Lindsay Smith, in: Metalloporphyrins in Catalytic Oxidations, R.A. Sheldon (Ed.) (M. Dekker, New York, 1994) p. 325.

[5] K. Miki and Y. Sato, Bull. Chem. Soc. Jpn. 66 (1993) 2385.

[6] J.E. Lyons and P.E. Ellis, Catal. Lett. 8 (1991) 45; M.W. Grinstaff, M.G. Hill, J.A. Labinger and H.B. Gray, Science 264 (1994) 1311; E. Bill, X. Ding, E.L. Bominaar, A.X. Trautwein, H. Winkler, D. Mandon, R. Weiss, A. Gold, K. Jayaraj, W.E. Hatfield and M.L. Kirk, Eur. J. Biochem. 188 (1990) 665; H. Sugimoto, H.C. Tung and D.T. Sawyer, J. Am. Chem. Soc. 110 (1988) 2465; D. Mandon, R. Weiss, K. Jayaraj, A. Gold, J. Terner, E. Bill and A.X. Trautwein, Inorg. Chem. 31 (1992) 4404; K. Yamaguchi, Y. Watanabe and I. Morishima, J. Chem. Soc. Chem. Commun. (1992) 1721; H. Fujii, J. Am. Chem. Soc. 115 (1993) 4641.

[7] A. Gold, K. Jayaraj, P. Doppelt, R. Weiss, G. Chottard, E. Bill, X. Ding and A.X. Trautwein, J. Am. Chem. Soc. 110 (1988) 5756.

[8] Y. Iamamoto, M.D. Assis, O. Baffa, S. Nakagaki and O.R. Nascimento, J. Inorg. Biochem. 52 (1993) 191.

[9] M.D. Assis, O.A. Serra, Y.Iamamoto and O.R. Nascimento, Inorg. Chim. Acta. 187 (1991) 107.

[10] S. Nakagaki, Y.Iamamoto, O. Baffa and O.R. Nascimento, Inorg. Chim. Acta 186 (1991) 39.

[11] A.D. Adler, F.R. Longo, F. Kampas and J. Kim, J. Inorg. Nucl. Chem. 32 (1970) 2443.

[12] O. Leal, D.L. Anderson, R.G. Bowman, F. Basolo and J. Burwell, Jr., J. Am. Chem. Soc. 97 (1975) 5125.

[13] J.G. Sharefkin and H. Saltzmann, Org. Synth. 43 (1963) 62.

[14] Y. Iamamoto, K.J. Ciuffi, H.C. Sacco, C.M.C. Prado, M. Moraes and O.R. Nascimento, J. Mol. Catal. 88 (1994) 167.

[15] Y. Iamamoto, K.J. Ciuffi, H.C. Sacco, L.S. Iwamoto, O.R. Nascimento and C.M.C. Prado, J. Mol. Catal., in press.

[16] R.J. Cheng, L. Latos-Grazynski and A.L. Balch, Inorg. Chem. 21 (1982) 2412; H. Kobayashi, T. Higuchi, Y. Kaizu, H. Osada and M. Aoki, Bull. Chem. Soc. Jpn. 48 (1975) 3137.

[17] J.P. Mahy, P. Battioni, G. Bedi, D. Mansuy, J. Fischer, R. Weiss and I. Morgenstern-Badarau, Inorg. Chem. 27 (1988) 353.

[18] J.T. Groves and Y. Watanabe. J. Am. Chem. Soc. 110 (1988) 8443.

[19] C.M. Dicken, P.N. Balasubramanian and T.C. Bruice, Inorg. Chem. 27 (1988) 197.

[20] Y. Iamamoto, M.D. Assis, K.J. Ciufi, H.C. Sacco, L.S. Iwamoto, A.J.B. Melo, O.R. Nascimento and C.M.C. Prado, J. Mol. Catal. 109 (1996) 189; M.D. Assis, A.J.B. Melo, O.A. Serra and Y. Iamamoto, J. Mol. Catal. A 97 (1995) 41.

[21] K. Jayaraj, A. Gold, G.E. Toney, J.H. Helms and W.E. Hatlield, Inorg. Chem. 25 (1986) 3516.

[22] K.J. Ciuffi, Master Dissertation, University of São Paulo, 1993, Ribeirão Preto, Brazil.

[23] R.H. Felton, G.S. Owen, D. Dolphin, A. Forman, D.C. Borg and J. Fajer, Ann. NY Acad. Sci. 206 (1973) 504; T.S. Calderwood, W.A. Lee and T.C. Bruice, J. Am. Chem. Soc. 103 (1985) 8272; Gold, K. Jayaraj, P. Doppelt, R. Weiss, G. Chottard, E. Bill, X. Ding and A.X. Trautwein, J. Am. Chem. Soc. 110 (1988) 5756.

[24] L. Martin Neto, O.R. Nascimento, M. Tabak and I. Caracelli, Biochim. Biophys. Acta 956 (1988) 189.

[25] L. Martin Neto, O.R. Nascimento and M. Tabak, J. Inorg. Biochem. 40 (1990) 309.
[26] P.R. Cooke, C. Gilmartin, G.W. Gray and J.R. Lindsay-Smith, J. Chem. Soc. Perkin Trans. 2 (1995) 1573.
[27] Y. Iamamoto, M.D. Assis, K.J. Ciuffi, C.M.C. Prado, B.Z. Prellwitz, M. Moraes, O.R. Nascimento and H.C. Sacco, J. Mol. Catal, in press.
[28] R.W. Lee, P.C. Nakagaki and T.C. Bruice, J. Am. Chem. Soc. 111 (1989) 1368.
[29] D. Ostovic, Gong-Xin Hen and T.C. Bruice, in: Metalloporphyrins in Catalytic Oxidations, R.A. Sheldon (Ed.) (M. Dekker, New York, 1994) p. 58.
[30] M. Gunter and P. Turner, J. Mol. Catal. 66 (1991) 121; P. Battioni, J.P. Renaud, J.F. Bartoli, M. Reina-Artiles, M. Fort and D. Mansuy, J. Am. Chem. Soc. 110 (1988) 8462; R.D. Arasasingham, Gong-Xin He and T.C. Bruice, J. Am. Chem. Soc. 115 (1993) 7985.
[31] P.R. Cooke and J.R. Lindsay-Smith, J. Chem. Soc. Perkin Trans. 1 (1994) 1913.